PHYSICAL REVIEW A VOLUME 39, NUMBER 2 JANUARY 15, 1989

SO(4) symmetry and the static Jahn-Teller effect in icosahedral molecules

A. Ceulemans
Department of Chemistry, University of Leuven, Celestijnenlaan 200F, B-3030 Leuven, Belgium

P. W. Fowler
Department of Chemistry, University of Exeter, Stocker Road, Exeter EX4 4QD, England
(Received 23 August 1988)

The $G\times(g+h)$ Jahn-Teller problem, relevant to the instability of icosahedral molecules in fourfold-degenerate electronic states, is investigated. The stationary points of the resulting adiabatic potential energy surface are retrieved by the method of the isostationary function. This method takes advantage of the parent SO(4) symmetry of the $G\times(g+h)$ problem under equal-coupling conditions. The structure of the surface depends on the relative strength of the coupling to fourfold- and fivefold-degenerate modes. If the $G\times g$ coupling is predominant, five tetrahedral minima are found, forming the vertices of a four-dimensional tetrahedron. If the $G\times h$ coupling is the more pronounced, ten trigonal minima are found at the vertices of a Petersen graph. The results are in agreement with the epikernel principle.

I. INTRODUCTION

The icosahedral orbital quadruplet G is Jahn-Teller (JT) active under nine vibrational coordinates, transforming according to the fourfold- and fivefold-degenerate representations $G\oplus H$. This JT problem is usually denoted as the $G\times(g+h)$ problem. Khlopin *et al.* have studied the five-dimensional $G\times h$ subsystem[1] but to date no general solution of the full system is available.[2]

In the present paper we determine the extremal points of the adiabatic potential energy surface (PES) for the full $G\times(g+h)$ Hamiltonian. Our analysis is based on the SO(4) parent symmetry of this Hamiltonian.[3]

II. ICOSAHEDRAL MOLECULES

Icosahedral molecules are comparatively rare in nature and their electronic states have been studied only sporadically.[4] However, the icosahedral B_{12} subunit dominates the structural chemistry of boron allotropes[5] and several examples of molecules with I_h or near-I_h symmetry are now known, including the largest *closo*-borane anion ($B_{12}H_{12}^{2-}$) (Ref. 6) and the recently synthesized hydrocarbon dodecahedrane ($C_{20}H_{20}$).[7] A truncated icosahedral structure of I_h symmetry has been proposed to explain the "C_{60}" signal in the mass spectrum of the products of laser vaporization of graphite[8] and theoretical studies of the millimeter-wave spectra of liquid water have considered a near-icosahedral $(H_2O)_{60}$ cluster.[9]

In the wake of the C_{60} hypothesis much effort was directed towards a qualitative understanding of the electronic structure of this and related species. It was shown that, in a simple Hückel picture, C_{60} would have a closed electronic shell with a large gap between the highest occupied molecular orbital (HOMO) and the lowest unoccupied molecular orbital (LUMO) and retain much of the π stabilization of graphite.[10] In fact, an infinite series of icosahedral carbon shells is theoretically possible, with at least one for each C_n where $n=20(b^2+bc+c^2)$ and $b\geq 0, c\geq 0$. Such clusters fall into two disjoint classes.[11] When $b-c$ is divisible by 3 the cluster has a multiple of 60 atoms and is closed shell. Otherwise, the number of atoms is $60k+20$ and the cluster has a closed shell only as the doubly charged cation C_n^{2+}. The neutral molecules of this second series have a G^2 configuration with two electrons occupying a fourfold-degenerate orbital (G, G_g, or G_u). The singly charged cations, C_n^+ with $n=60k+20$, have a fourfold-degenerate ground state and thus should exemplify a $G\times(g+h)$-type JT instability.

The parent member of the first series is the truncated icosahedral C_{60} molecule. Simple geometrical arguments show that a closed-shell neutral molecule can be expected for any $n=60+6m$ ($m=0,2,3,\ldots$) whether the symmetry is icosahedral or not.[12] Each cluster has 12 pentagonal faces and all other faces hexagonal.

If twenty carbon atoms are placed at the vertices of the regular dodecahedron (symmetry I_h) they form the simplest possible cluster with 12 pentagonal faces, C_{20}. This is the prototype of the $60k+20$ icosahedral series and as a neutral molecule would have the π configuration $(A_g)^2(T_{1u})^6(H_g)^{10}(G_u)^2$. The I_h C_{20}^{2+} cation occupies at least a local minimum on the potential energy hypersurface [as shown by exploratory *ab initio* self-consistent-field (SCF) calculations[13]], but clearly the singly charged cation C_{20}^+ must distort to a lower symmetry by the Jahn-Teller theorem. In all probability the low-spin ground state of the neutral species will exhibit the same type of distortion. One interesting aspect of the general algebraic treatment in the present paper is that it provides guidance as to how a molecule with a G-type HOMO would distort and what elements of symmetry would be lost in the process.

III. SYMMETRY ASPECTS

In the subsequent treatment extensive use will be made of the finite and infinite invariance groups of the

$G\times(g+h)$ problem. This section is concerned with a precise definition of the various symmetry transformations involved. Three levels of symmetry are considered: the infinite SO(4) group, the finite icosahedral group at the JT origin, and the icosahedral subgroups which result from the symmetry-lowering distortions.

A. Parent SO(4) group

As has been demonstrated by Pooler,[14,15] SO(4) is an invariance group of the $G\times(g+h)$ system *under equal coupling conditions*. The concept which lies behind the use of such continuous groups for Jahn-Teller systems is the degeneracy space of the electronic manifold.[3] If this manifold is to be related to a finite group representation of the first kind, as is the case for the icosahedral G representation, the degeneracy space may be taken to be real. This real space of the electronic quadruplet may be described by a fixed set of four orthogonal unit vectors, $\{|Ga\rangle,|Gx\rangle,|Gy\rangle,|Gz\rangle\}$. An arbitrary function, $|G\gamma\rangle$, can be expressed by means of four direction cosines, say a, x, y, and z, referring to the four angles between $|G\gamma\rangle$ and the respective unit vectors,

$$|G\gamma\rangle=a|Ga\rangle+x|Gx\rangle+y|Gy\rangle+z|Gz\rangle \quad (1)$$
$$\text{with } a^2+x^2+y^2+z^2=1 .$$

Alternatively, one could use hyperspherical polar coordinates r,χ,θ,φ as in Eq. (2).[16]

$$\left.\begin{aligned} x&=r\cos\varphi\sin\theta\sin\chi\\ y&=r\sin\varphi\sin\theta\sin\chi\\ z&=r\cos\theta\sin\chi\\ a&=r\cos\chi \end{aligned}\right\} \text{with } r=1;\ 0\le\varphi\le 2\pi;\ 0\le\theta\le\pi;\ 0\le\chi\le\pi . \quad (2)$$

The polar forms of the corresponding gradient and Hessian operators[17] are given in Appendix A.

The normalized row vector (a,x,y,z) defines a point on the unit hypersphere around the origin of the electronic space. The group of proper rotations of this vector is the special orthogonal group in four dimensions, SO(4). In view of the subsequent applications, we briefly recall the local properties of SO(4). The four coordinates give rise to six generators:[18,19]

$$\begin{aligned} \mathcal{J}_{xa}&=-i\left[x\frac{\partial}{\partial a}-a\frac{\partial}{\partial x}\right],\\ \mathcal{J}_{ya}&=-i\left[y\frac{\partial}{\partial a}-a\frac{\partial}{\partial y}\right],\\ \mathcal{J}_{za}&=-i\left[z\frac{\partial}{\partial a}-a\frac{\partial}{\partial z}\right], \quad (3)\\ \mathcal{J}_{yz}&=-i\left[y\frac{\partial}{\partial z}-z\frac{\partial}{\partial y}\right],\\ \mathcal{J}_{zx}&=-i\left[z\frac{\partial}{\partial x}-x\frac{\partial}{\partial z}\right],\\ \mathcal{J}_{xy}&=-i\left[x\frac{\partial}{\partial y}-y\frac{\partial}{\partial x}\right]. \end{aligned}$$

These generators obey the commutation relations in Eq. (4)

$$\begin{aligned} &[\mathcal{J}_{tu},\mathcal{J}_{tv}]=i\mathcal{J}_{uv} ,\\ &[\mathcal{J}_{tu},\mathcal{J}_{vw}]=0 , \end{aligned} \quad (4)$$

where t, u, v, and w are distinct Cartesian coordinates.

Symmetry-adapted forms of these operators are given in Eq. (5):

$$\begin{aligned} \mathcal{J}_{1x}&=\tfrac{1}{2}(\mathcal{J}_{xa}+\mathcal{J}_{yz}) ,\\ \mathcal{J}_{1y}&=\tfrac{1}{2}(\mathcal{J}_{ya}+\mathcal{J}_{zx}) ,\\ \mathcal{J}_{1z}&=\tfrac{1}{2}(\mathcal{J}_{za}+\mathcal{J}_{xy}) , \quad (5)\\ \mathcal{J}_{2x}&=\tfrac{1}{2}(\mathcal{J}_{xa}-\mathcal{J}_{yz}) ,\\ \mathcal{J}_{2y}&=\tfrac{1}{2}(\mathcal{J}_{ya}-\mathcal{J}_{zx}) ,\\ \mathcal{J}_{2z}&=\tfrac{1}{2}(\mathcal{J}_{za}-\mathcal{J}_{xy}) . \end{aligned}$$

The $\mathcal{J}_1$ and $\mathcal{J}_2$ operators in Eq. (5) are the angular-momentum operators of two independent SO(3) factor groups of SO(4). In consequence, an irreducible representation of SO(4) may be labeled by a pair of j quantum numbers as (j_1,j_2). Such a representation has dimension $(2j_1+1)(2j_2+1)$. Representations will be integer if j_1 and j_2 are both integer or both half-integer. The tensorial rank of a (j_1,j_2) representation is equal to the sum of its j values.

The coordinate functions a,x,y,z were defined as the natural action space of SO(4). Accordingly, these components span the fundamental "vectorial" or "canonical" representation of SO(4), with $j_1=j_2=\frac{1}{2}$. This may easily be verified by applying the Casimir operators $\mathcal{J}_1^2$ and $\mathcal{J}_2^2$ to the coordinate functions. As an example one has for a

$$\begin{aligned} \mathcal{J}_1^2 a&=(\mathcal{J}_{1x}^2+\mathcal{J}_{1y}^2+\mathcal{J}_{1z}^2)a\\ &=\tfrac{1}{4}(\mathcal{J}_{xa}^2+\mathcal{J}_{ya}^2+\mathcal{J}_{za}^2)a\\ &=\tfrac{3}{4}a . \end{aligned} \quad (6)$$

In turn, the transformation properties of the $\mathcal{J}$ operators are to be determined from their commutation relations. As an example, combination of Eqs. (3)–(5) yields

$$[\mathscr{J}_{1z},\mathscr{J}_{1x}\pm i\mathscr{J}_{1y}]=\pm(\mathscr{J}_{1x}\pm i\mathscr{J}_{1y}) ,$$
$$[\mathscr{J}_{2z},\mathscr{J}_{1x}\pm i\mathscr{J}_{1y}]=0 . \tag{7}$$

These commutation relations show that the three $\mathscr{J}_1$ components transform like $j_1=1, j_2=0$, and thus form a basis for the (1,0) representation. Likewise, the three components of $\mathscr{J}_2$ may be shown to span the (0,1) representation.

B. Icosahedral group

The finite symmetry group of the quadruplet problem is the icosahedral group I_h. Since the Jahn-Teller active vibrations are of even parity, the centrosymmetry of the icosahedron cannot be destroyed and the problem may be examined equally well in the framework of the icosahedral rotation group I. Figure 1 shows the numbering of the symmetry operations of I in a Cartesian reference frame.

Our conventions follow precisely the recommendations of Boyle and Parker.[20] The symmetry axes $\mathcal{C}_5^{1,12}$ and $\mathcal{C}_3^{1,4,3}$ are generators of I. Other generator elements of interest are $\mathcal{C}_3^{1,4,3}$ and $\mathcal{C}_2^{1,2}$ for the tetrahedral rotational subgroup T, $\mathcal{C}_3^{1,2,3}$ and $\mathcal{C}_2^{4,5}$ for D_3, and $\mathcal{C}_2^{1,2}$ and $\mathcal{C}_2^{4,5}$ for D_2.

Boyle and Parker have also specified a suitable standard choice of irreducible representations. Their canonical components will be labeled a,x,y,z for G and $\theta,\epsilon,\xi,\eta,\zeta$ for H. The defining transformation matrices for relevant generators are given in Appendix B. Furthermore, a complete set of Clebsch-Gordan (CG) coupling coefficients for the Boyle-Parker symmetry basis has been published recently.[21]

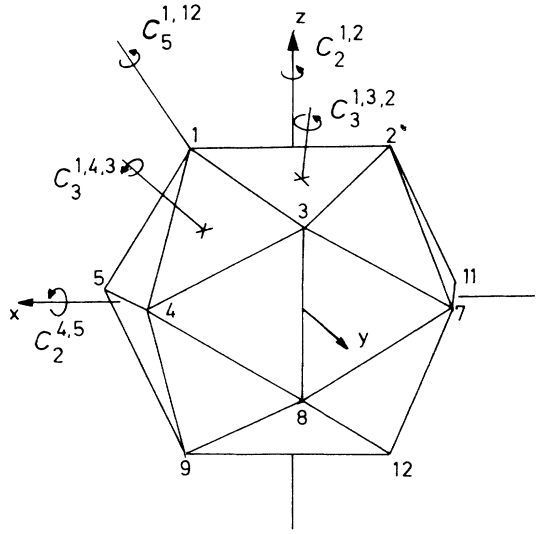

FIG. 1. Icosahedral symmetry group in a Cartesian reference frame, according to the conventions of Boyle and Parker (Ref. 20). Various useful generators of the icosahedral subgroups are also indicated.

The representation matrices of G form a faithful representation of I and in addition have determinant $+1$. The icosahedral group may thus be embedded in SO(4). The subduction table for the SO(4)$\downarrow I$ symmetry lowering can be obtained by standard procedures. An interesting illustration in the recent literature is offered by the subduction of SO(4) to the hyperoctahedral group SW_4.[22,23]

Table I shows the splitting of the SO(4) representations (j_1,j_2) up to the fourth rank. Evidently, the scalar representation (0,0) will correspond to the totally symmetric representation A of I. Similarly, the vectorial representation $(\frac{1}{2},\frac{1}{2})$ corresponds to the symmetry of the degeneracy space and thus subduces G. The operator representations (1,0) and (0,1) are threefold degenerate and thus must subduce T_1 or T_2. A precise assignment of their icosahedral transformation properties may be obtained by coupling two G vectors, (a,x,y,z) and $(\partial/\partial a,\partial/\partial x,\partial/\partial y,\partial/\partial z)$, to a T_1 product. From the tabulated CG coupling coefficients[21] one finds

TABLE I. Decomposition of irreducible (j_1,j_2) representations of SO(4) to irreducible representations of I.

j_1+j_2	(j_1,j_2)	dim	
0	(0,0)	1	A
1	(1,0)	3	T_2
	(0,1)	3	T_1
	$(\frac{1}{2},\frac{1}{2})$	4	G
2	(2,0)	5	H
	(0,2)	5	H
	$(\frac{3}{2},\frac{1}{2})$	8	T_1+H
	$(\frac{1}{2},\frac{3}{2})$	8	T_2+H
	(1,1)	9	$G+H$
3	(3,0)	7	T_1+G
	(0,3)	7	T_2+G
	$(\frac{5}{2},\frac{1}{2})$	12	T_2+G+H
	$(\frac{1}{2},\frac{5}{2})$	12	T_1+G+H
	(2,1)	15	T_1+T_2+G+H
	(1,2)	15	T_1+T_2+G+H
	$(\frac{3}{2},\frac{3}{2})$	16	$A+T_1+T_2+G+H$
4	(4,0)	9	$G+H$
	(0,4)	9	$G+H$
	$(\frac{7}{2},\frac{1}{2})$	16	$A+T_1+T_2+G+H$
	$(\frac{1}{2},\frac{7}{2})$	16	$A+T_1+T_2+G+H$
	(3,1)	21	$A+T_1+T_2+G+2H$
	(1,3)	21	$A+T_1+T_2+G+2H$
	$(\frac{5}{2},\frac{3}{2})$	24	$T_1+T_2+2G+2H$
	$(\frac{3}{2},\frac{5}{2})$	24	$T_1+T_2+2G+2H$
	(2,2)	25	$A+T_1+T_2+2G+2H$

$$T_{1x}=\frac{1}{2}\left[a\frac{\partial}{\partial x}-x\frac{\partial}{\partial a}+y\frac{\partial}{\partial z}-z\frac{\partial}{\partial y}\right],$$
$$T_{1y}=\frac{1}{2}\left[a\frac{\partial}{\partial y}-y\frac{\partial}{\partial a}-x\frac{\partial}{\partial z}+z\frac{\partial}{\partial x}\right], \quad (8)$$
$$T_{1z}=\frac{1}{2}\left[a\frac{\partial}{\partial z}-z\frac{\partial}{\partial a}+x\frac{\partial}{\partial y}-y\frac{\partial}{\partial x}\right].$$

Upon substitution it may easily be verified that the T_1 tensor in Eq. (8), multiplied by i, coincides with the $\mathcal{J}_2$ operator in Eq. (5). Hence the (0,1) representation of $\mathcal{J}_2$ transforms as T_1. Likewise, the (1,0) representation of $\mathcal{J}_1$ may be shown to transform as T_2.[24] Further relations follow from a comparison of analogous Kronecker products in both groups. As an example, one has

$$(\tfrac{1}{2},\tfrac{1}{2})\otimes(\tfrac{1}{2},\tfrac{1}{2})=[(0,0)\oplus(1,1)]\oplus\{(1,0)\oplus(0,1)\},$$
$$G\otimes G=[A\oplus G\oplus H]\oplus\{T_1\oplus T_2\}. \quad (9)$$

Since the (0,0), (1,0) and (0,1) representations in Eq. (9) have already been assigned unambiguously, it follows that the (1,1) representation must subduce the remaining $G\oplus H$ representation. This is the symmetry spanned by the JT active coordinates.

The square of the coordinate representation (1,1) produces *inter alia* the (2,2) representation, which is a symmetrized representation of the fourth rank,

$$(1,1)\otimes(1,1)$$
$$=[(0,0)\oplus(1,1)\oplus(0,2)\oplus(2,0)\oplus(2,2)]$$
$$\oplus\{(1,0)\oplus(0,1)\oplus(2,1)\oplus(1,2)\}. \quad (10)$$

This (2,2) representation is of special importance, since it yields a totally symmetric icosahedral component, which determines the PES of the $G\times(g+h)$ problem [see below Eq. (18)]. Repetition of this procedure will eventually generate the entire subduction table.

C. Epikernel and kernel subgroups

JT distorting forces acting along nontotally symmetric vibrational modes will carry the nuclei over into configurations corresponding to subgroup symmetries of the parent icosahedral group. The lowest subgroup attainable for a particular mode, is called the *kernel* of that mode. Allowed intermediate subgroups are termed *epikernels*.[25,26] The kernel and epikernels are determined uniquely by the symmetry representations of the distortion modes. They are most easily obtained by inspection of a descent-in-symmetry sequence of the parent point group.[26] In such a sequence, the symmetry-lowering capacity of a given distortion mode will be used up as soon as a subgroup is reached which leaves the total mode representation invariant. This subgroup corresponds to the kernel endpoint. Between the parent group, where the entire representation is nontotally symmetric, and the kernel, where total invariance is reached, there is usually a gradual increase in the number of invariant components: each *first appearance* of a new invariant component in this chain marks an epikernel subgroup.

This procedure will now be illustrated for the JT-active G and H vibrations. The relevant subduction scheme[27] is shown in Fig. 2. Clearly, for both representations the kernel corresponds to the trivial subgroup C_1. This is the first subgroup for which the G and H representations become totally invariant. Likewise, the epikernels may be determined from the first appearances of A_1 (or A) components along the various descent routes. As an example, consider the decomposition of H along the pentagonal chain:

$$\begin{array}{lllll} I\rightarrow D_5 & & \rightarrow C_5 & & \rightarrow C_1 \\ H\rightarrow \mathcal{A}_1+E_1+E_2 & \rightarrow & \mathcal{A}+E_1+E_2 & \rightarrow & 5\mathcal{A}. \end{array} \quad (11)$$

In this chain D_5 is an epikernel, but C_5 is not. Indeed D_5 marks the first appearance of an A_1 component, while no additional invariance arises under C_5. As another example, the C_2 subgroup is seen to yield more invariant H components than any of the preceding subgroups [cf. Eq. (12)]. Hence C_2 must be an epikernel of H,

$$\begin{array}{lll} D_2: & 2\mathcal{A}+B_1+B_2+B_3 & \\ D_3: & \mathcal{A}_1+2E & \rightarrow C_2: \ 3\mathcal{A}+2B. \\ D_5: & \mathcal{A}_1+E_1+E_2 & \end{array} \quad (12)$$

In this way all the attainable subgroups of G and H vibrations may be determined. The results are represented in Table II. The same procedure may also be applied to the total nine-dimensional coordinate representation $G\oplus H$.

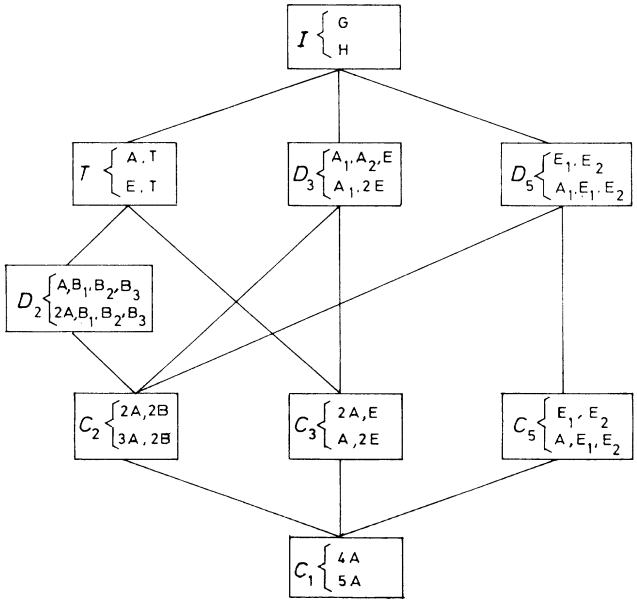

FIG. 2. Genealogy of the icosahedral rotation group, including the subduction chains for the G and H representations.

TABLE II. Kernel and epikernel subgroups for the fourfold- and fivefold-degenerate representations of I.

Representation[a]	Kernel	Epikernels
G	C_1	T, D_3, C_3, C_2
H	C_1	D_5, D_3, D_2, C_2
(G,H)	C_1	D_3, D_2, C_3, C_2

[a](G,H) refers to configurations that are obtained by combinations of G and H displacements.

As before, each increase in the number of invariant components of the sum representation as a whole marks an epikernel of $G \oplus H$. In the present example all the epikernels of $G \oplus H$ are found to be epikernels of one or both of the irreducible representations involved.

From Fig. 2 and Table II, the epikernel groups of G and H are seen to give rise to chains of consecutive subgroups. The first members of these chains immediately below I are the epikernels T, D_3, and D_5. These epikernels are also referred to as the *maximal epikernels.* D_2 is a subgroup of T and therefore must be considered as a lower ranking epikernel. C_2 and C_3 are still at a lower level, just before the kernel tail. In our subsequent treatment the maximal epikernels will be of primary importance.

IV. MODEL HAMILTONIAN

In this section we consider the model Hamiltonian $\mathcal{H}$, that generates the $G \times (g+h)$ surface. As has been shown by Khlopin *et al.*,[1] the extremal properties of this surface are independent of the number of interacting fourfold- and fivefold-degenerate modes. The electronic Hamiltonian may therefore be restricted to the ideal single-mode limit, with only one vibrational mode of G and one of H symmetry. $\mathcal{H}$ is written as follows:

$$\mathcal{H} = \mathcal{H}^0 + \sum_{\Lambda,\lambda} \left[\frac{\partial \mathcal{H}}{\partial Q_{\Lambda\lambda}} \right]_0 Q_{\Lambda\lambda} + \tfrac{1}{2} \sum_{\Lambda,\lambda} K_\Lambda Q_{\Lambda\lambda}^2 \ . \tag{13}$$

Here $Q_{\Lambda\lambda}$ denotes one of the nine JT-active coordinates. K_Λ is the harmonic force constant of the Λ mode. The zero refers to the icosahedral starting configuration. Usually this icosahedral origin is placed at zero energy. The action of $\mathcal{H}$ in the electronic quadruplet space generates an adiabatic potential energy surface, with four sheets, $E_k(Q)$, as expressed in Eq. (14):

$$E_k(Q) = \tfrac{1}{2} \sum_{\Lambda,\lambda} K_\Lambda Q_{\Lambda\lambda}^2 + \epsilon_k(Q), \quad k = 1,2,3,4 \tag{14}$$

where $\epsilon_k(Q)$ is the kth root of the secular equation:

$$\| W_{ij}(Q) - \epsilon_k(Q) \delta_{ij} \| = 0 \ , \tag{15}$$

with

$$W_{ij}(Q) = \sum_{\Lambda,\lambda} \left\langle Gi \left| \frac{\partial \mathcal{H}}{\partial Q_{\Lambda\lambda}} \right| Gj \right\rangle_0 Q_{\Lambda\lambda} = \sum_{\Lambda,\lambda} F_\Lambda Q_{\Lambda\lambda} \langle Gi | \Lambda\lambda Gj \rangle \ .$$

$\mathbb{W}$ is a force element matrix, describing the linear distorting forces which destabilize the JT origin. F_Λ is the irreducible force element for vibration of symmetry type Λ. The bracket denotes the appropriate CG coupling coefficient; i and j represent components of the electronic representation G. The explicit expressions for the elements of $\mathbb{W}$ may be derived from the published CG tables[21] and are given in Eqs. (16):

$$\begin{aligned}
W_{aa} &= \frac{\sqrt{3}}{2} F_G Q_a \ , \\
W_{xx} &= -\frac{1}{2\sqrt{3}} F_G Q_a + \frac{\sqrt{2}}{\sqrt{15}} F_H (-Q_\theta + \sqrt{3} Q_\epsilon) \ , \\
W_{yy} &= -\frac{1}{2\sqrt{3}} F_G Q_a + \frac{\sqrt{2}}{\sqrt{15}} F_H (-Q_\theta - \sqrt{3} Q_\epsilon) \ , \\
W_{zz} &= -\frac{1}{2\sqrt{3}} F_G Q_a + \frac{2\sqrt{2}}{\sqrt{15}} F_H Q_\theta \ , \\
W_{ax} &= W_{xa} = -\frac{1}{2\sqrt{3}} F_G Q_x + \frac{1}{\sqrt{3}} F_H Q_\xi \ , \\
W_{ay} &= W_{ya} = -\frac{1}{2\sqrt{3}} F_G Q_y + \frac{1}{\sqrt{3}} F_H Q_\eta \ , \\
W_{az} &= W_{za} = -\frac{1}{2\sqrt{3}} F_G Q_z + \frac{1}{\sqrt{3}} F_H Q_\zeta \ , \\
W_{xy} &= W_{yx} = -\frac{\sqrt{5}}{2\sqrt{3}} F_G Q_z - \frac{1}{\sqrt{15}} F_H Q_\zeta \ , \\
W_{xz} &= W_{zx} = -\frac{\sqrt{5}}{2\sqrt{3}} F_G Q_y - \frac{1}{\sqrt{15}} F_H Q_\eta \ , \\
W_{yz} &= W_{zy} = -\frac{\sqrt{5}}{2\sqrt{3}} F_G Q_x - \frac{1}{\sqrt{15}} F_H Q_\xi \ .
\end{aligned} \tag{16}$$

Here Q_a, Q_x, Q_y, Q_z are the four G-type coordinates and $Q_\theta, Q_\epsilon, Q_\xi, Q_\eta, Q_\zeta$ are the five H-type coordinates, obeying the standard transformation properties, as specified in Appendix B. For further use we define also in Eq. (17) the JT stabilization energies[3] for both modes, $E_G^{\rm JT}$ and $E_H^{\rm JT}$:

$$\begin{aligned}
E_G^{\rm JT} &= -\frac{3}{8} \frac{F_G^2}{K_G} \ , \\
E_H^{\rm JT} &= -\frac{3}{10} \frac{F_H^2}{K_H} \ .
\end{aligned} \tag{17}$$

Previously Khlopin, Polinger, and Bersuker[1] derived the stationary points of the adiabatic JT surface for the special case of zero JT stabilization energy along the G mode, i.e., $E_G^{\rm JT} = 0$. In this case JT activity is restricted to the subspace of the five H coordinates.

Another special solution arises if the JT stabilization energies for both modes are *equal.* In this instance the surface may be shown to consist of an equipotential energy trough surrounding the JT origin.[3,28,29] This trough extends in the nine-dimensional coordinate space and has three degrees of freedom. It exhibits the rotational invariance of the hypersphere, a change of direction in the electronic space being related to an equipotential displacement on the bottom of the trough.

The most general case with unequal JT stabilization

energies for G and H modes may be viewed as the result of symmetry breaking of this rotational invariance.[3] In this process the adiabatic surface retains a continuous minimal energy trough, though no longer of uniform depth. A warping occurs, giving rise to the appearance of minima, local hill tops, and saddle points.

These extremal points may easily be found with the guidance of the *epikernel principle*.[3,26] According to this principle extremal points on a JT surface are expected to be associated with epikernel symmetries. More specifically, stable minima prefer maximal epikernel symmetries.

In the present work we will use a different method, based on the *isostationary function*.[3] This method evaluates the symmetry-breaking properties of the JT Hamiltonian with respect to the parent SO(4) group. It allows one to locate all the extrema of the $G\times(g+h)$ surface. At the same time it provides a useful check on the validity of the epikernel principle for icosahedral molecules.

V. LOCALIZATION OF EXTREMAL POINTS

The problem we are facing is to find the extremal points of a nine-dimensional surface, described by the roots of a secular equation. For a linear model Hamiltonian this problem may be solved in two steps.[3] The first step consists in finding the extremal eigenvectors by minimizing the so-called isostationary function in four-dimensional electronic space. In the second step these extremal eigenvectors are inserted in the stationary conditions of Oepik and Pryce,[30] to yield the distortion coordinates of the extremal points.

A. Isostationary function

The isostationary function, $\langle\|E\|\rangle$, is a function of the electronic coordinates a,x,y,z, specified in Eq. (1). It is stationary for the eigenvectors of the extremal points on the JT surface. For a two-mode problem, such as the $G\times(g+h)$ problem, $\langle\|E\|\rangle$ consists of a scalar term, which is the weighted average of the JT stabilization energies of the two modes, and a tensorial term, which contains the icosahedral invariants of the symmetrized fourth rank representation of SO(4), with $j_1=j_2=2$. Inspection of Table I reveals that this (2,2) representation yields only one totally symmetric component upon subduction from SO(4) to I. Denoting this component as $f^{A}_{2,2}$, one may write

$$\langle\|E\|\rangle=\tfrac{4}{9}E_G^{\mathrm{JT}}+\tfrac{5}{9}E_H^{\mathrm{JT}}+\tfrac{20}{27}(E_G^{\mathrm{JT}}-E_H^{\mathrm{JT}})f^{A}_{2,2}\ . \tag{18}$$

The $f^{A}_{2,2}$ function is given by

$$f^{A}_{2,2}=\tfrac{3}{20}[16a^4-12a^2+1]-\tfrac{3}{2}[x^4+y^4+z^4-\tfrac{3}{5}(x^2+y^2+z^2)^2]+\frac{18}{\sqrt{5}}axyz \quad \text{with } a^2+x^2+y^2+z^2=1\ . \tag{19}$$

This expression for $f^{A}_{2,2}$ was obtained by using the general formula of Ref. 3, in combination with the Clebsch-Gordan coefficients, tabulated in Ref. 21. A detailed derivation[31] is presented in Appendix C. The same result can also be achieved by using the technique of the so-called integrity basis.[32]

For equal JT stabilization energies ($E_G^{\mathrm{JT}}=E_H^{\mathrm{JT}}$), the term in $f^{A}_{2,2}$ vanishes and the value of the isostationary function is constant everywhere in electronic space. This corresponds to the degenerate coupling case, which gives rise to an equipotential minimal energy trough in the actual JT distortion space. For unequal JT stabilization energies the stationary points of $\langle\|E\|\rangle$ may be found by minimizing the $f^{A}_{2,2}$ function, subject to the eigenvector normalization condition. The use of Lagrange multipliers yields 80 extremal eigenvectors. Since $f^{A}_{2,2}$ is an even function under spatial inversion, all eigenvectors occur in pairs with opposite sign. In this way 40 nontrivial eigenvectors remain, as listed in Table III. The *symmetry* of an extremal eigenvector is the group of all symmetry operations of I which either leave this eigenvector invariant or change its sign. As an example, the (1,0,0,0) eigenvector is clearly invariant under the generators of the T subgroup. Hence it has tetrahedral symmetry. The group T is also said to be the *stabilizer* of the (1,0,0,0) point.[33] As a further example the eigenvector $(1/\sqrt{6},-\sqrt{5}/\sqrt{6},0,0)$ is stabilized by $\mathcal{C}_3^{1,2,3}$ and $\mathcal{C}_2^{4,5}$ and therefore has D_3 symmetry. Finally, the (0,1,0,0) eigenvector is found to be invariant under the $\mathcal{C}_2^{4,5}$ axis. It changes to $(0,-1,0,0)$ under $\mathcal{C}_2^{1,2}$. Hence the stabilizer of this eigenvector contains both perpendicular $\mathcal{C}_2$ axes and therefore is identified as D_2.

The *orbit* of a pair of antipodal eigenvectors is defined as the set of antipodal pairs that are mapped onto each other by elements of I.[33] The 40 pairs of extremal eigenvectors are found to be separable into four orbits, labeled as $\alpha,\beta,\gamma,\delta$ with respective symmetries T_d,D_3,D_3,D_2. The number of elements in a given orbit is equal to the quotient of the orders of parent and stabilizing groups, as required by the orbit-stabilizer theorem.[34] Hence one has

$$\begin{aligned}&\dim\alpha=\dim I/\dim T=5\ ,\\ &\dim\beta=\dim\gamma=\dim I/\dim D_3=10\ ,\\ &\dim\delta=\dim I/\dim D_2=15\ .\end{aligned} \tag{20}$$

Finally, the *nature* of an extremum may be found by evaluating the Hessian matrix, as defined in Appendix A. All eigenvectors of a given orbit are symmetry equivalent and thus will have the same Hessian eigenvalues. The results are specified in Table IV.

For a dominant JT stabilization along the G mode, i.e., $E_G^{\mathrm{JT}}<E_H^{\mathrm{JT}}<0$, the α points with tetrahedral symmetry have three positive Hessian eigenvalues, which is characteristic of a true minimum. In the β points the isostationary function has an overall negative curvature, which points to a maximum. If, on the other hand, the H mode is more stabilized than the G mode, i.e., for $E_H^{\mathrm{JT}}<E_G^{\mathrm{JT}}<0$, these assignments must be reversed and the trigonal β points correspond to the minima. The remaining γ and δ points are always saddle points of index 1 or 2. These conclusions are also apparent from the extremal values of the isostationary function itself. Clearly, for dominant $G\times g$ coupling the $\langle\|E\|\rangle$ energy function reaches its

TABLE III. Extremel eigenvectors of the isostationary function for the $G\times(g+h)$ problem. Eigenvectors are denoted as (a,x,y,z). Only one eigenvector of each antipodal pair $\pm(a,x,y,z)$ is listed.

α:T	β:D_3	γ:D_3	δ:D_2
$(1,0,0,0)$	$\frac{1}{\sqrt{6}}(1,-\sqrt{5},0,0)$	$\frac{1}{\sqrt{2}}(0,0,1,-1)$	$(0,1,0,0)$
$\frac{1}{4}(1,\sqrt{5},\sqrt{5},\sqrt{5})$	$\frac{1}{\sqrt{6}}(1,\sqrt{5},0,0)$	$\frac{1}{\sqrt{2}}(0,0,1,1)$	$(0,0,1,0)$
$\frac{1}{4}(1,\sqrt{5},-\sqrt{5},-\sqrt{5})$	$\frac{1}{\sqrt{6}}(1,0,-\sqrt{5},0)$	$\frac{1}{\sqrt{2}}(0,1,0,-1)$	$(0,0,0,1)$
$\frac{1}{4}(1,-\sqrt{5},\sqrt{5},-\sqrt{5})$	$\frac{1}{\sqrt{6}}(1,0,\sqrt{5},0)$	$\frac{1}{\sqrt{2}}(0,1,0,1)$	$\frac{1}{4}(\sqrt{5},1,1,-3)$
$\frac{1}{4}(1,-\sqrt{5},-\sqrt{5},\sqrt{5})$	$\frac{1}{\sqrt{6}}(1,0,0,-\sqrt{5})$	$\frac{1}{\sqrt{2}}(0,1,-1,0)$	$\frac{1}{4}(\sqrt{5},1,-1,3)$
	$\frac{1}{\sqrt{6}}(1,0,0,\sqrt{5})$	$\frac{1}{\sqrt{2}}(0,1,1,0)$	$\frac{1}{4}(\sqrt{5},-1,1,3)$
	$\frac{1}{2\sqrt{6}}(3,-\sqrt{5},-\sqrt{5},-\sqrt{5})$	$\frac{1}{2\sqrt{2}}(\sqrt{5},1,1,1)$	$\frac{1}{4}(\sqrt{5},-1,-1,-3)$
	$\frac{1}{2\sqrt{6}}(3,-\sqrt{5},\sqrt{5},\sqrt{5})$	$\frac{1}{2\sqrt{2}}(\sqrt{5},1,-1,-1)$	$\frac{1}{4}(\sqrt{5},1,3,-1)$
	$\frac{1}{2\sqrt{6}}(3,\sqrt{5},-\sqrt{5},\sqrt{5})$	$\frac{1}{2\sqrt{2}}(\sqrt{5},-1,1,-1)$	$\frac{1}{4}(\sqrt{5},1,-3,1)$
	$\frac{1}{2\sqrt{6}}(3,\sqrt{5},\sqrt{5},-\sqrt{5})$	$\frac{1}{2\sqrt{2}}(\sqrt{5},-1,-1,1)$	$\frac{1}{4}(\sqrt{5},-1,3,1)$
			$\frac{1}{4}(\sqrt{5},-1,-3,-1)$
			$\frac{1}{4}(\sqrt{5},3,1,-1)$
			$\frac{1}{4}(\sqrt{5},3,-1,1)$
			$\frac{1}{4}(\sqrt{5},-3,1,1)$
			$\frac{1}{4}(\sqrt{5},-3,-1,-1)$

minimum in the tetrahedral α points, while the $G\times h$ coupling favors the stabilization of the trigonal β points.

B. Distortion coordinates of the extremal points

Oepik and Pryce have obtained stationary conditions for the coordinates of the extremal points by minimizing the secular equation with respect to each distortion coordinate:[20]

$$[a,x,y,z]\begin{bmatrix}\frac{\partial \mathbb{W}}{\partial Q_{\Lambda\lambda}}\end{bmatrix}\begin{bmatrix}a\\x\\y\\z\end{bmatrix}+K_\Lambda Q_{\Lambda\lambda}=0 \quad \text{for all } \Lambda\lambda\in G\oplus H \ . \tag{21}$$

TABLE IV. Symmetry, energy, and extremal characteristics of the four orbits of stationary eigenvectors. The JT stabilization energies, $E_G^{\rm JT}$ and $E_H^{\rm JT}$, are defined in Eq. (17).

orbit	dim	symmetry	$\langle\|E\|\rangle$	Hessian eigenvalues[a]		
α	5	T	$E_G^{\rm JT}$	-6	-6	-6
β	10	D_3	$\frac{2}{27}E_G^{\rm JT}+\frac{25}{27}E_H^{\rm JT}$	$+2$	$+2$	$+8$
γ	10	D_3	$\frac{2}{3}E_G^{\rm JT}+\frac{1}{3}E_H^{\rm JT}$	-6	-6	$\frac{24}{5}$
δ	15	D_2	$\frac{1}{9}E_G^{\rm JT}+\frac{8}{9}E_H^{\rm JT}$	$+6$	$+6$	$-\frac{6}{5}$

[a]All values are to be multiplied by $\frac{20}{27}(E_G^{\rm JT}-E_H^{\rm JT})$.

The explicit forms of these conditions are given by

$$
\begin{aligned}
Q_a &= -\frac{F_G}{2\sqrt{3}K_G}(3a^2-x^2-y^2-z^2)\,,\\
Q_x &= \frac{F_G}{\sqrt{3}K_G}(ax+\sqrt{5}yz)\,,\\
Q_y &= \frac{F_G}{\sqrt{3}K_G}(ay+\sqrt{5}xz)\,,\\
Q_z &= \frac{F_G}{\sqrt{3}K_G}(az+\sqrt{5}xy)\,,\\
Q_\theta &= -\frac{\sqrt{2}F_H}{\sqrt{15}K_H}(2z^2-x^2-y^2)\,,\\
Q_\epsilon &= -\frac{\sqrt{2}F_H}{\sqrt{5}K_H}(x^2-y^2)\,,\\
Q_\xi &= \frac{2F_H}{\sqrt{15}K_H}(-\sqrt{5}ax+yz)\,,\\
Q_\eta &= \frac{2F_H}{\sqrt{15}K_H}(-\sqrt{5}ay+xz)\,,\\
Q_\zeta &= \frac{2F_H}{\sqrt{15}K_H}(-\sqrt{5}az+xy)\,.
\end{aligned}
\tag{22}
$$

In these expressions the electronic eigenvectors are coupled to a traceless second-rank tensor, which may be seen to form a basis for the (1,1) representation of SO(4). [See Table I and Eq. (9)]. This representation does indeed subduce the $G\oplus H$ symmetry species of the distortion coordinates. Extremum coordinates, $\|Q_{\Lambda\lambda}\|$, may be found by introducing in Eq. (22) the extremal eigenvectors, listed in Table III. Since the (1,1) coordinate representation is of even rank, eigenvectors of opposite sign give rise to the same coordinates and thus refer to the same extremum point in coordinate space. The four orbits of eigenvectors yield four types of stationary points. One representative of each type is described in Table V. The other equivalent points may be found by inserting the other eigenvectors of the same orbit or by applying symmetry operations of I. Table V also provides expressions for the eigenvectors and eigenvalues of the excited G components at each extremum point. The corresponding splitting patterns are displayed in Fig. 3. From the figure and the table, it is clear that the two different types of D_3 extrema refer to different symmetry assignments of the nondegenerate ground-state component.

The conclusions of Sec. V A regarding the extremal nature of the various types of solutions may be checked by explicitly evaluating the local curvature of the JT surface at the stationary points. As an example we analyze the curvature in the tetrahedral point, specified in Table V. A perturbation theoretic expansion of the secular equation[30] for the relevant (1,0,0,0) eigenvector yields to second order:

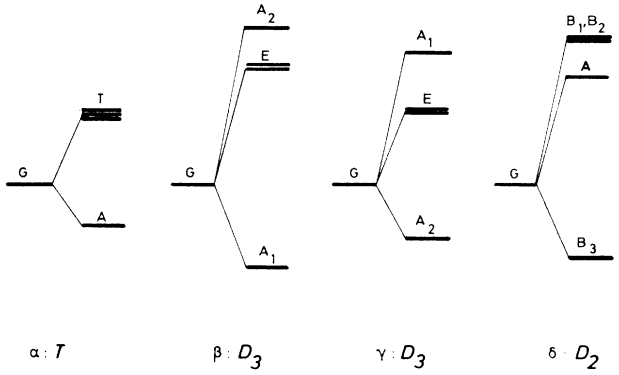

FIG. 3. Splitting of the electronic quadruplet for the various types of extrema. The energy levels were calculated from the expressions in Table V, assuming $E_G^{\rm JT}=\frac{1}{2}E_H^{\rm JT}$. This case corresponds to a trigonal minimum (β:D_3), with A_1 ground state.

$$
\begin{aligned}
E_1(Q) \approx & -\frac{3}{8}\frac{F_G^2}{K_G}+\tfrac{1}{2}K_G(Q_a-\|Q_a\|)^2+\tfrac{1}{2}K_H(Q_\theta^2+Q_\epsilon^2)\\
&+\tfrac{1}{2}(Q_x,Q_\xi)(\mathbb{F})\begin{bmatrix}Q_x\\Q_\xi\end{bmatrix}\\
&+\tfrac{1}{2}(Q_y,Q_\eta)(\mathbb{F})\begin{bmatrix}Q_y\\Q_\eta\end{bmatrix}\\
&+\tfrac{1}{2}(Q_z,Q_\zeta)(\mathbb{F})\begin{bmatrix}Q_z\\Q_\zeta\end{bmatrix}\,,
\end{aligned}
\tag{23}
$$

with

$$
\|Q_a\| = -\frac{\sqrt{3}}{2}\frac{F_G}{K_G}\,,
$$

$$
\mathbb{F} = \begin{bmatrix} \frac{5}{6}K_G & \frac{1}{3}K_G\frac{F_H}{F_G} \\ \frac{1}{3}K_G\frac{F_H}{F_G} & K_H-\frac{2}{3}K_G\frac{F_H^2}{F_G^2}\end{bmatrix}\,.
$$

Equation (23) represents a quadratic potential energy expression which yields nine local normal modes of $A+E+2T$ symmetry. The corresponding force constants are given in Table VI. The K_A and K_E force constants are seen to be positive so that the A and E modes always represent directions of positive curvature. In contrast, one of the K_T constants reaches a value of zero for $E_G^{\rm JT}=E_H^{\rm JT}$. This case corresponds to the special solution of degenerate coupling, which is characterized by a flat equipotential trough. The T mode at zero frequency will be tangent to the bottom of this trough. For $E_G^{\rm JT}<E_H^{\rm JT}<0$ both K_T constants may be verified to be positive. This confirms the previous conclusion that for a dominant JT stabilization along the G mode, the tetrahedral points will be true minima. On the other hand, for $E_H^{\rm JT}<E_G^{\rm JT}<0$ one of the K_T force constants is

TABLE V. Ground-state and excited components, energies, and extremal coordinates for a representation solution of each symmetry type.

Symmetry	Eigenvectors		Energy	$\|Q_G\|$ (units of F_G/K_G) (Q_a,Q_x,Q_y,Q_z)	$\|Q_H\|$ (units of F_H/K_H) $(Q_\theta,Q_\epsilon,Q_\xi,Q_\eta,Q_\zeta)$
α:$T(C_3^{1,4,3},C_2^{1,2})$	(1,0,0,0)	A	E_G^{JT}	$\left[-\frac{\sqrt{3}}{2},0,0,0\right]$	(0,0,0,0,0)
	(0,1,0,0) (0,0,1,0) (0,0,0,1)	T	$-\frac{5}{3}E_G^{\mathrm{JT}}$		
β:$D_3(C_3^{1,3,2},C_2^{4,5})$	$\frac{1}{\sqrt{6}}(1,-\sqrt{5},0,0)$	A_1	$\frac{2}{27}E_G^{\mathrm{JT}}+\frac{25}{27}E_H^{\mathrm{JT}}$	$\left[\frac{1}{6\sqrt{3}},\frac{-\sqrt{5}}{6\sqrt{3}},0,0\right]$	$\left[\frac{\sqrt{5}}{3\sqrt{6}},-\frac{\sqrt{5}}{3\sqrt{2}},\frac{\sqrt{5}}{3\sqrt{3}},0,0\right]$
	$\frac{1}{2\sqrt{2}}(-\sqrt{5},-1,1,1)$ $\frac{1}{2\sqrt{6}}(\sqrt{5},1,3,3)$	E	$-\frac{10}{27}E_G^{\mathrm{JT}}-\frac{35}{27}E_H^{\mathrm{JT}}$		
	$\frac{1}{\sqrt{2}}(0,0,1,-1)$	A_2	$\frac{10}{27}E_G^{\mathrm{JT}}-\frac{55}{27}E_H^{\mathrm{JT}}$		
γ:$D_3(C_3^{1,3,2},C_2^{4,5})$	$\frac{1}{\sqrt{2}}(0,0,1,-1)$	A_2	$\frac{2}{3}E_G^{\mathrm{JT}}+\frac{1}{3}E_H^{\mathrm{JT}}$	$\left[\frac{1}{2\sqrt{3}},\frac{-\sqrt{5}}{2\sqrt{3}},0,0\right]$	$\left[-\frac{1}{\sqrt{30}},\frac{1}{\sqrt{10}},-\frac{1}{\sqrt{15}},0,0\right]$
	$\frac{1}{2\sqrt{2}}(-\sqrt{5},-1,1,1)$ $\frac{1}{2\sqrt{6}}(\sqrt{5},1,3,3)$	E	$-\frac{14}{9}E_G^{\mathrm{JT}}-\frac{1}{9}E_H^{\mathrm{JT}}$		
	$\frac{1}{\sqrt{6}}(0,-\sqrt{5},0,0)$	A_1	$-\frac{2}{9}E_G^{\mathrm{JT}}-\frac{13}{9}E_H^{\mathrm{JT}}$		
δ:$D_2(C_2^{1,2},C_2^{4,5})$	(0,1,0,0)	B_3	$\frac{1}{9}E_G^{\mathrm{JT}}+\frac{8}{9}E_H^{\mathrm{JT}}$	$\left[\frac{1}{2\sqrt{3}},0,0,0\right]$	$\left[\frac{\sqrt{2}}{\sqrt{15}},-\frac{\sqrt{2}}{\sqrt{5}},0,0,0\right]$
	(1,0,0,0)	A	$-\frac{7}{9}E_G^{\mathrm{JT}}-\frac{8}{9}E_H^{\mathrm{JT}}$		
	(0,0,1,0) (0,0,0,1)	B_2 B_1	$\frac{1}{9}E_G^{\mathrm{JT}}-\frac{16}{9}E_H^{\mathrm{JT}}$		

TABLE VI. Local normal modes and force constants for the tetrahedral extremum.

Normal mode	Force constant[a]
A:$Q_a-\|Q_a\|$	K_G
E: Q_θ, Q_ϵ	K_H
T: (Q_x,Q_ξ), (Q_y,Q_η), (Q_z,Q_ζ)	$X[1\pm(1+Y)^{1/2}]$

[a] X and Y are defined as follows:

$$X=\tfrac{5}{12}K_G+K_H\left[\frac{1}{2}-\frac{5}{12}\frac{E_H^{\mathrm{JT}}}{E_G^{\mathrm{JT}}}\right],$$

$$Y=\frac{F_H^2K_G}{4X^2}\left[\frac{1}{E_H^{\mathrm{JT}}}-\frac{1}{E_G^{\mathrm{JT}}}\right].$$

bound to be negative, thus indicating that the tetrahedral points are no longer stabilized.

The results from Table V may also be compared with the previous study of the separate $G\times h$ problem by Khlopin *et al.*[1] In the absence of JT stabilization along the G mode ($F_G=0$) the tetrahedral distortions will no longer be activated, since they are confined to the coordinate space of G symmetry. However, the three other types of extrema will remain and their components in H space may be shown to coincide with the results of Ref. 1.

VI. DISCUSSION

A. $G\times g$ versus $G\times h$ coupling

The adiabatic surface of the linear $G\times(g+h)$ problem may adopt two different forms depending on which of the two participating modes gives rise to the larger JT stabilization energy. If the stabilization along the G mode is more pronounced, the surface will be characterized by

five equivalent tetrahedral minima, forming the α orbit. Next in energy to these minima are the ten D_3 extrema, described by the γ orbit. For $E_G^{JT} < E_H^{JT} < 0$, these extrema are saddle points of index 1 (see Table IV) and therefore correspond to transition states between two neighboring tetrahedral minima. Furthermore, evaluation of the distances between various extremal points in coordinate space reveals that the five tetrahedral minima are all at equal distance from each other. The topology of this tetrahedron based surface may thus be represented by the completely connected pentagraph, as shown in Fig. 4. This complete five-graph is isomorphous to the four-dimensional tetrahedron. It has ten edges, that match the ten D_3 transition states of the γ orbit. Tunneling between the five T minima will give rise to two vibronic energy levels of $A+G$ symmetry.

If on the other hand, the stabilization energy for the H mode is larger, the surface will be characterized by the ten D_3 minima of the β orbit. Next in energy for this coupling regime are the 15 D_2 extrema of the δ orbit. For $E_H^{JT} < E_G^{JT} < 0$ these extrema appear to be saddle points of index 1 (see Table IV) and therefore will act as transition states between two neighboring D_3 minima. Distance calculations reveal that every D_3 minimum is adjacent to three equivalent nearest neighbors and at equal distance from the six remaining D_3 minima. The topology of this surface may be described by the so-called *Petersen* graph,[35] with ten vertices for the β orbit and 15 edges for the transition states of the δ orbit (see Fig. 5). In such a graph two different isomerization pathways are conceivable, involving either adjacent or nonadjacent minima. Interestingly, the same graph may also be used to represent a particular isomerization mode of a trigonal bipyramid.[36] Finally we note that tunneling between the ten D_3 minima will give rise to three vibronic energy levels of $A+G+H$ symmetry.

B. Validity of the epikernel principle

As may be seen from Table II and the ensuing discussion in Sec. III the $G \oplus H$ distortion space contains three maximal epikernel subgroups: T, D_5, and D_3. According to the epikernel principle[3,26] these are likely to be associated with stable minima of the adiabatic potential energy surface. From this list the D_5 epikernel must be eliminated, since a D_5 distortion splits the electronic manifold into two degenerate components, E_1+E_2, and thus is unable to remove the electronic degeneracy. The remaining T and D_3 epikernels (T_h and D_{3d} for centrosymmetric problems) were indeed found to characterize the two possible types of minima.

The situation is comparable to the linear $T \times (e+t_2)$ problem in cubic symmetry.[26,28] This problem is also characterized by only two maximal epikernels: D_3 and D_4. If $T \times e$ coupling is dominant, minima adopt the tetragonal epikernel symmetry of the E mode. On the other hand, a $T \times t_2$ coupling regime stabilizes points with the trigonal epikernel symmetry of the T_2 mode. There is a slight difference though in that the D_3 maximal epikernel of the $G \oplus H$ distortion space is not confined to the irreducible subspace of the H mode, but consists of both G and H components.

Furthermore, the method of the isostationary function has revealed the presence of subsidiary stationary points with D_3 and D_2 epikernel symmetries. It is conceivable that these points may become absolute minima as a result of second-order interactions. Finally, the lower-ranking epikernels, C_3 and C_2, and the C_1 kernel itself, do not give rise to stationary points of the linear hamiltonian. These conclusions confirm the validity of the epikernel principle for icosahedral JT problems.

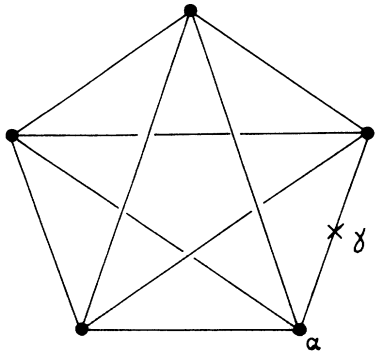

FIG. 4. Topology of the JT surface for preferential $G \times g$ coupling. The five vertices of the graph represent the five tetrahedral minima (α), while the ten edges refer to isomerization paths over trigonal transition states (γ).

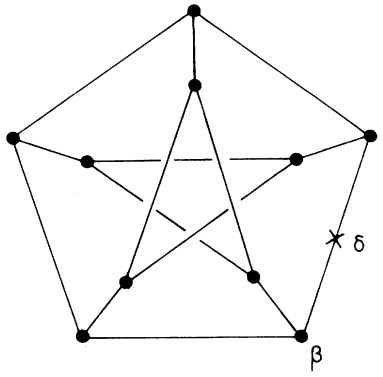

FIG. 5. Topology of the JT surface for preferential $G \times h$ coupling. The ten vertices of the graph represent the ten trigonal minima (β), while the 15 edges refer to isomerization paths over D_2 transition states (δ).

ACKNOWLEDGMENTS

We thank L. L. Boyle for a stimulating discussion. The work was supported by a research grant from the Belgian Government (Programmatie van het Wetenschapsbeleid). A. C. thanks the Belgian National Science Foundation (NFWO) for financial support.

APPENDIX A: GRADIENT, LAPLACIAN, AND HESSIAN IN HYPERSPHERICAL POLAR COORDINATES

The relationship between rectilinear (a,x,y,z) and polar (r,χ,θ,φ) coordinates is given in Eq. (2) of Sec. III A. The polar components of the four-dimensional gradient have been given by Louck.[16] One has

$$\begin{aligned}\nabla_r &= \frac{\partial}{\partial r}\ ,\\ \nabla_\chi &= \frac{1}{r}\frac{\partial}{\partial \chi}\ ,\\ \nabla_\theta &= \frac{1}{r\sin\chi}\frac{\partial}{\partial \theta}\ ,\\ \nabla_\varphi &= \frac{1}{r\sin\chi\sin\theta}\frac{\partial}{\partial \varphi}\ .\end{aligned} \tag{A1}$$

Hence the total gradient is

$$\nabla = \left[\mathbf{e}_r\frac{\partial}{\partial r}, \mathbf{e}_\chi\frac{1}{\tau}\frac{\partial}{\partial \chi}, \mathbf{e}_\theta\frac{1}{r\sin\chi}\frac{\partial}{\partial \theta}, \mathbf{e}_\varphi\frac{1}{r\sin\theta\sin\chi}\frac{\partial}{\partial \varphi}\right]. \tag{A2}$$

Here the e's represent the unit vectors in the polar coordinate system. They are related to the rectilinear unit vectors by the following expressions:

$$\begin{aligned}\mathbf{e}_r &= \cos\chi\mathbf{e}_a + \sin\chi\cos\theta\mathbf{e}_z + \sin\chi\sin\theta\sin\varphi\mathbf{e}_y\\ &\quad + \sin\chi\sin\theta\cos\varphi\mathbf{e}_x\ ,\\ \mathbf{e}_\chi &= -\sin\chi\mathbf{e}_a + \cos\chi\cos\theta\mathbf{e}_z + \cos\chi\sin\theta\sin\varphi\mathbf{e}_y\\ &\quad + \cos\chi\sin\theta\cos\varphi\mathbf{e}_x\ ,\\ \mathbf{e}_\theta &= -\sin\theta\mathbf{e}_z + \cos\theta\sin\varphi\mathbf{e}_\varphi + \cos\theta\cos\varphi\mathbf{e}_x\ ,\\ \mathbf{e}_\varphi &= \cos\varphi\mathbf{e}_y - \sin\varphi\mathbf{e}_x\ .\end{aligned} \tag{A3}$$

Now to obtain the $\nabla\nabla$ tensor, we follow the same procedure as Stone.[17] From Eq. (A3) the appropriate derivatives of the polar unit vectors may easily be evaluated. One has

$$\begin{bmatrix}\frac{\partial}{\partial r}\\ \frac{\partial}{\partial \chi}\\ \frac{\partial}{\partial \theta}\\ \frac{\partial}{\partial \varphi}\end{bmatrix}(\mathbf{e}_r\mathbf{e}_\chi\mathbf{e}_\theta\mathbf{e}_\varphi) = \begin{bmatrix} 0 & 0 & 0 & 0\\ e_\chi & -\mathbf{e}_r & 0 & 0\\ \sin\chi\mathbf{e}_\theta & \cos\chi\mathbf{e}_\theta & -\cos\chi\mathbf{e}_\chi - \sin\chi\mathbf{e}_r & 0\\ \sin\chi\sin\theta\mathbf{e}_\varphi & \cos\chi\sin\theta\mathbf{e}_\varphi & \cos\theta\mathbf{e}_\varphi & -\sin\theta\sin\chi\mathbf{e}_r - \sin\theta\cos\chi\mathbf{e}_\chi - \cos\theta\mathbf{e}_\theta\end{bmatrix}. \tag{A4}$$

$$\nabla\nabla = \begin{bmatrix} \frac{\partial^2}{\partial r^2} & \frac{\partial}{\partial r}\frac{1}{r}\frac{\partial}{\partial \chi} & \frac{\partial}{\partial r}\frac{1}{r\sin\chi}\frac{\partial}{\partial \theta} & \frac{\partial}{\partial r}\frac{1}{r\sin\chi\sin\theta}\frac{\partial}{\partial \varphi}\\ \frac{\partial}{\partial r}\frac{1}{r}\frac{\partial}{\partial \chi} & \frac{1}{r}\frac{\partial}{\partial r} + \frac{1}{r^2}\frac{\partial^2}{\partial \chi^2} & \frac{\partial}{\partial \chi}\frac{1}{r^2\sin\chi}\frac{\partial}{\partial \theta} & \frac{\partial}{\partial \chi}\frac{1}{r^2\sin\chi\sin\theta}\frac{\partial}{\partial \varphi}\\ \frac{\partial}{\partial r}\frac{1}{r\sin\chi}\frac{\partial}{\partial \theta} & \frac{\partial}{\partial \chi}\frac{1}{r^2\sin\chi}\frac{\partial}{\partial \theta} & \frac{1}{r}\frac{\partial}{\partial r} + \frac{1}{r^2\sin^2\chi}\frac{\partial^2}{\partial \theta^2} + \frac{\cot\chi}{r^2}\frac{\partial}{\partial \chi} & \frac{\partial}{\partial \theta}\frac{1}{r^2\sin^2\chi\sin\theta}\frac{\partial}{\partial \varphi}\\ \frac{\partial}{\partial r}\frac{1}{r\sin\chi\sin\theta}\frac{\partial}{\partial \varphi} & \frac{\partial}{\partial \chi}\frac{1}{r^2\sin\chi\sin\theta}\frac{\partial}{\partial \theta\varphi} & \frac{\partial}{\partial \theta}\frac{1}{r^2\sin^2\chi\sin\theta}\frac{\partial}{\partial \varphi} & \frac{1}{r}\frac{\partial}{\partial r} + \frac{1}{r^2\sin^2\chi\sin^2\theta}\frac{\partial^2}{\partial \varphi^2} + \frac{\cot\chi}{r^2}\frac{\partial}{\partial \chi} + \frac{\cot\theta}{r^2\sin^2\chi}\frac{\partial}{\partial \theta} \end{bmatrix} \tag{A5}$$

The trace of this tensor corresponds to the polar form of the four-dimensional Laplacian:

$$\nabla^2 = \frac{\partial^2}{\partial r^2} + \frac{1}{r^2}\frac{\partial^2}{\partial \chi^2} + \frac{1}{r^2\sin^2\chi}\frac{\partial^2}{\partial \theta^2} + \frac{1}{r^2\sin^2\chi\sin^2\theta}\frac{\partial^2}{\partial \varphi^2} + \frac{3}{r}\frac{\partial}{\partial r} + \frac{2\cot\chi}{r^2}\frac{\partial}{\partial \chi} + \frac{\cot\theta}{r^2\sin^2\chi}\frac{\partial}{\partial \theta}\ . \tag{A6}$$

The second derivatives on the surface of the four-dimensional unit sphere are readily obtained from Eq. (A5) by setting

r equal to 1. Accordingly the surface Hessian of a function f is given by Eq. (A7). Here $f_\varphi=\partial f/\partial\varphi$, $f_{\chi\theta}=\partial^2 f/\partial\chi\partial\theta$, etc.,

$$\nabla\nabla|_{r=1}f=\begin{bmatrix} f_{\chi\chi} & \frac{1}{\sin\chi}f_{\chi\theta}-\frac{\cos\chi}{\sin^2\chi}f_\theta & \frac{1}{\sin\chi\sin\theta}f_{\chi\varphi}-\frac{\cos\chi}{\sin^2\chi\sin\theta}f_\varphi \\ \frac{1}{\sin\chi}f_{\chi\theta}-\frac{\cos\chi}{\sin^2\chi}f_\theta & \frac{1}{\sin^2\chi}f_{\theta\theta}+\cot\chi f_\chi & \frac{1}{\sin^2\chi\sin\theta}f_{\theta\varphi}-\frac{\cos\theta}{\sin^2\chi\sin^2\theta}f_\varphi \\ \frac{1}{\sin\chi\sin\theta}f_{\chi\varphi}-\frac{\cos\chi}{\sin^2\chi\sin\theta}f_\varphi & \frac{1}{\sin^2\chi\sin\theta}f_{\theta\varphi}-\frac{\cos\theta}{\sin^2\chi\sin^2\theta}f_\varphi & \frac{1}{\sin^2\chi\sin^2\theta}f_{\varphi\varphi}+\cot\chi f_\chi+\frac{\cot\theta}{\sin^2\chi}f_\theta \end{bmatrix} . \tag{A7}$$

APPENDIX B: TRANSFORMATION MATRICES FOR THE G REPRESENTATION

Boyle and Parker[20] have listed a few representative matrices describing the transformation of the G components under the symmetry elements $\mathcal{C}_5^{1,12},\mathcal{C}_3^{1,4,3},\mathcal{C}_2^{1,2}$ of I, as specified in Fig. 1. For convenience these matrices are repeated here, together with the matrices for the $\mathcal{C}_3^{1,3,2}$ and $\mathcal{C}_2^{4,5}$ generator elements of D_3. In our conventions[21] symmetry transformations are defined as follows:

$$\mathcal{R}(a,x,y,z)=(a,x,y,z)[(\mathbb{D}(\mathcal{R})] . \tag{B1}$$

The $\mathbb{D}(\mathcal{R})$ matrices in Eq. (B1) are transposed, as compared to the matrices of Boyle and Parker. Following the convention of Eq. (B1), one has

$$\mathbb{D}(\mathcal{C}_5^{1,12})=\begin{bmatrix} -1/4 & -\sqrt{5}/4 & \sqrt{5}/4 & \sqrt{5}/4 \\ \sqrt{5}/4 & -3/4 & -1/4 & -1/4 \\ \sqrt{5}/4 & 1/4 & -1/4 & 3/4 \\ -\sqrt{5}/4 & -1/4 & -3/4 & 1/4 \end{bmatrix} , \tag{B2}$$

$$\mathbb{D}(\mathcal{C}_3^{1,4,3})=\begin{bmatrix} 1&0&0&0 \\ 0&0&0&1 \\ 0&1&0&0 \\ 0&0&1&0 \end{bmatrix} , \tag{B3}$$

$$\mathbb{D}(\mathcal{C}_3^{1,3,2})=\begin{bmatrix} -1/4 & -\sqrt{5}/4 & -\sqrt{5}/4 & -\sqrt{5}/4 \\ -\sqrt{5}/4 & 3/4 & -1/4 & -1/4 \\ \sqrt{5}/4 & 1/4 & 1/4 & -3/4 \\ \sqrt{5}/4 & 1/4 & -3/4 & 1/4 \end{bmatrix} , \tag{B4}$$

$$\mathbb{D}(\mathcal{C}_2^{1,2})=\begin{bmatrix} 1&0&0&0 \\ 0&-1&0&0 \\ 0&0&-1&0 \\ 0&0&0&1 \end{bmatrix} , \tag{B5}$$

$$\mathbb{D}(\mathcal{C}_2^{4,5})=\begin{bmatrix} 1&0&0&0 \\ 0&1&0&0 \\ 0&0&-1&0 \\ 0&0&0&-1 \end{bmatrix} . \tag{B6}$$

APPENDIX C: ICOSAHEDRAL INVARIANT OF THE (2,2) REPRESENTATION OF SO(4)

The function $f_{2,2}^A$ represents the icosahedral invariant of the fourth-rank irreducible tensor representation of SO(4). It may be derived in a straightforward way, using Eq. (26) of Ref. 3. According to this equation, one has

$$f_{2,2}^A=\sum_{i,j,k,l} a_i a_j a_k a_l T_{ijkl} . \tag{C1}$$

Here i, j, k, and l run independently from 1 to 4, with $a_1=a$, $a_2=x$, $a_3=y$, and $a_4=z$. The T elements involve summations over Clebsch-Gordan coefficients:

$$T_{ijkl}=\sum_{g\in G}\langle Ga_i|GgGa_j\rangle\langle Ga_k Gg|Ga_l\rangle - \sum_{h\in H}\langle Ga_i|HhGa_j\rangle\langle Ga_k Hh|Ga_l\rangle . \tag{C2}$$

In evaluating these expressions, the permutational symmetry of the tabulated CG coefficients[21] is seen to give rise to the following simplifying relationships:

$$T_{ijkl}=T_{jikl}=T_{ijlk}=T_{jilk} =T_{klij}=T_{lkij}=T_{klji}=T_{lkji} . \tag{C3}$$

In this way one obtains

$$f_{2,2}^A=\tfrac{3}{4}a^4-\tfrac{9}{20}(x^4+y^4+z^4)+\tfrac{21}{10}(x^2y^2+x^2z^2+y^2z^2) -\tfrac{3}{2}(a^2x^2+a^2y^2+a^2z^2)+\frac{18}{\sqrt{5}}axyz . \tag{C4}$$

With the use of the normalization condition, $a^2+x^2+y^2+z^2=1$, this expression may be rearranged to yield the functional form of Eq. (19). This form clearly shows the familiar tetrahedral invariants in x, y, and z that are contained in $f_{2,2}^A$. The first term in Eq. (19) is the Gegenbauer polynomial of order 4.[31]

[1]V. P. Khlopin, V. Z. Polinger, and I. B. Bersuker, Theor. Chim. Acta (Berlin) **48**, 87 (1978).

[2]For a survey of the extensive literature of the Jahn-Teller effect, see I. B. Bersuker, *The Jahn-Teller Effect, a Bibliographic Review* (Plenum, New York, 1984).

[3]A. Ceulemans, J. Chem. Phys. **87**, 5374 (1987).

[4]L. L. Boyle, Int. J. Quantum Chem. **6**, 919 (1972).

[5]N. N. Greenwood and A. Earnshaw, *Chemistry of the Elements* (Pergamon, New York, 1984).

[6]M. F. Hawthorne and A. R. Pittochelli, J. Am. Chem. Soc. **82**, 3228 (1960).

[7]R. J. Ternansky, D. W. Balogh, and L. A. Paquette, J. Am. Chem. Soc. **104**, 4503 (1982).

[8]H. W. Kroto, J. R. Heath, S. C. O'Brien, R. F. Curl, and R. E. Smalley, Nature **318**, 162 (1985).

[9]I. P. Buffey, W. Byers Brown, and H. A. Gebbie, Chem. Phys. Lett. **148**, 281 (1988).

[10]A. D. J. Haymet, Chem. Phys. Lett. **122**, 421 (1985).

[11]P. W. Fowler, Chem. Phys. Lett. **131**, 444 (1986).

[12]P. W. Fowler and J. I. Steer, J. Chem. Soc. Chem. Commun. 1403 (1987).

[13]P. W. Fowler, P. Lazzeretti, and R. Zanasi (unpublished).

[14]D. R. Pooler, J. Phys. A **11**, 1045 (1978).

[15]D. R. Pooler, J. Phys. C **13**, 1029 (1980).

[16]J. D. Louck, J. Mol. Spectrosc. **4**, 298 (1960).

[17]A. J. Stone, Mol. Phys. **41**, 1339 (1980).

[18]Here we follow the conventions of Ref. 19, which rotate the (a,x,y,z) vectors but leave the basis functions $\{|Ga\rangle,|Gx\rangle,|Gy\rangle,|Gz\rangle\}$ invariant.

[19]C. E. Wulfman, in *Recent Advances in Group Theory and their Application to Spectroscopy,* Vol. B43 of *Nato Advanced Study Institute: Series B, Physics,* edited by J. C. Donini (Plenum, New York, 1979), p. 329.

[20]L. L. Boyle and Yvonne M. Parker, Mol. Phys. **39**, 95 (1980). In the appendix of this reference, the second element in the third row of the C_5 matrix for T_1 is misprinted and should read $-\frac{1}{2}$.

[21]P. W. Fowler and A. Ceulemans, Mol. Phys. **54**, 767 (1985).

[22]M. Baake, B. Gemuenden, and R. Oedingen, J. Math. Phys. **23**, 944 (1982).

[23]M. Baake, B. Gemuenden, and R. Oedingen, J. Math. Phys. **24**, 1021 (1983).

[24]Pooler (Ref. 15) assigns T_1 to (1,0), and T_2 to (0,1). In view of our Eq. (8) this assignment seems erroneous.

[25]P. Murray-Rust, Buergi H.-B., and J. D. Dunitz, Acta Crystallo., Sec. A **A35**, 703 (1979).

[26]A. Ceulemans, D. Beyens, and L. G. Vanquickenborne, J. Am. Chem. Soc. **106**, 5824 (1983). Equation 10 of this reference contains several typographic errors: the bilinear terms in $Q_\theta Q_\xi$ and $Q_\theta Q_\eta$ should both have a minus sign; in the second row the term $\frac{1}{4}Q_\xi^2$ should read $\frac{1}{4}Q_\xi^2$; in the sixth row the term $X_t Q_\xi Q_\eta$ should read $X_t Q_\xi Q_\eta$.

[27]Suitable correlation tables may be found in P. Pelikán and M. Breza, J. Mol. Struct. (Theochem) **124**, 231 (1985).

[28]Mary C. M. O'Brien, Phys. Rev. **187**, 407 (1969).

[29]B. R. Judd, Can. J. Phys. **52**, 999 (1974).

[30]U. Oepik and M. H. L. Pryce, Proc. R. Soc. London **238**, 425 (1957).

[31]J. D. Talman, *Special Functions* (Benjamin, New York, 1968), Chap. 10.

[32]J. Patera and R. T. Sharp, in *Recent Advances in Group Theory and their Application to Spectroscopy,* Vol. B43 of *NATO Advanced Study Institute: Series B, Physics,* edited by J. C. Donini (Plenum, New York, 1979), p. 219.

[33]A. Ceulemans, Mol. Phys. **54**, 161 (1985).

[34]G. A. Jones and E. K. Lloyd, *Studies in Physical and Theoretical Chemistry,* edited by R. B. King (Elsevier, Amsterdam, 1983), Vol. 28, p. 252.

[35]C. Berge, *Graphs and Hypergraphs* (North-Holland, Amsterdam, 1973), p. 223.

[36]J. Brocas, M. Gielen, and R. Willem, *The Permutational Approach to Dynamic Stereochemistry* (McGraw-Hill, New York, 1983), p. 647.